Natural Hazards (2021) 106:2519–2544
https://doi.org/10.1007/s11069-021-04553-8

ORIGINAL PAPER

Debris flow magnitude, frequency, and precipitation threshold in the eastern North Cascades, Washington, USA

Jon L. Riedel[1] · **Sharon M. Sarrantonio**[1]

Received: 15 June 2020 / Accepted: 19 January 2021 / Published online: 23 February 2021

Abstract

We examine the magnitude, frequency, and precipitation threshold of the extreme flood hazard on 37 low-order streams in the lower Stehekin River Valley on the arid eastern slope of the North Cascades. Key morphometric variables identify the magnitude of the hazard by differentiating debris flood from debris flow systems. Thirty-two debris flow systems are fed by basins < 6 km^2 and deposited debris cones with slopes > 10°. Five debris flood systems have larger drainage areas and debris fans with slopes 7–10°. The debris flood systems have Melton ruggedness ratios from 0.42–0.64 compared to 0.78–3.80 for debris flow basins. We record stratigraphy at seven sites where soil surfaces buried by successive debris flows limit the age of events spanning 6000 years. Eighteen radiocarbon ages from the soils are the basis for estimates of a 200 to1500-year range in recurrence interval for larger debris flows and a 450 ± 50-year average. Smaller events occur approximately every 100 years. Fifteen debris flows occurred in nine drainage systems in the last 15 years, including multiple flows on three streams. Summer storms in 2010 and 2013 with peak rainfall intensities of 7–9 mm/h sustained for 8–11 h triggered all but one flow; the fall 2015 event on Canyon Creek occurred after 170 mm of rain in 78 h. A direct link between fires and debris flows is unclear because several recent debris flows occurred in basins that did not burn or burned at low intensity, and basins that burned at high intensity did not carry debris flows. All but one of the recent flows and fires occurred on the valley's southwest-facing wall. We conclude that fires and debris flows are linked by aspect at the landscape scale, where the sunny valley wall has flashy runoff due to sparse vegetation from frequent fires.

Keywords Debris flow hazard · Frequency · Precipitation threshold · Cascades

✉ Jon L. Riedel
Jon_Riedel@nps.gov

[1] U.S. National Park Service, Marblemount, USA

1 Introduction

Debris flows are rapid landslides consisting of large amounts of water, sediment, and woody debris, and present considerable hazards in mountain environments (Varnes 1978; Clague and Eisbacher 1984). They are particularly destructive because they can attain speeds of 13–15 m/s, depths of many meters, and can rapidly deposit tens of thousands of cubic meters of debris (Cruden and Varnes 1996). Globally, debris flows claimed 77,000 lives from 1950 to 2011 (Dowling and Santi 2014).

Debris flows vary widely, depending on the type of sediment and amount of water they carry, ranging from debris floods to viscous flows dominated by mud, gravel, woody debris, and boulders (Clague and Eisbacher 1984; Hungr et al. 2014). Most extreme flood events go through a range of flow types depending on the amount of sediment entrained, from floods to debris floods to debris flows. Debris floods represent extreme fluvial transport with 20–60% sediment by volume, while debris flows consist of more than 60% sediment (Beverage and Culbertson 1964; Pierson 2005). Debris flows are particularly hazardous because discharge can reach up to 40 times that of floods and many times larger than debris floods (Hungr et al. 2001). Mudflows are a type of debris flow dominated by silt and clay, while granular flows include boulders and cobbles. Coarse sediment and large woody debris deposited in larger streams by debris flows influence channel morphology and aquatic habitat (Swanson and Lienkaemper 1978; Benda 1985; Benda and Dunne 1997).

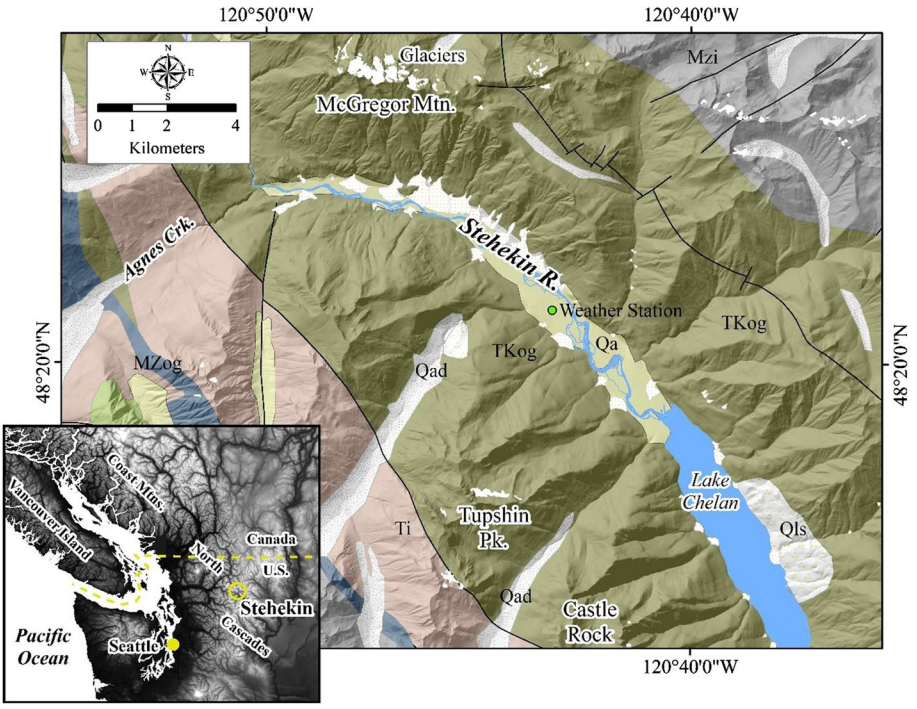

Fig. 1 Geology of the lower Stehekin River Valley and upper Lake Chelan. Map units include gneiss (Tkog and Mzog), tertiary granite (Ti), mesozoic granite (Mzi), quaternary alluvium (Qa) including debris cones, alpine glacial deposits (Qad), and landslides (Qls). Thin black lines are faults. Source Tabor and Haugerud (1999)

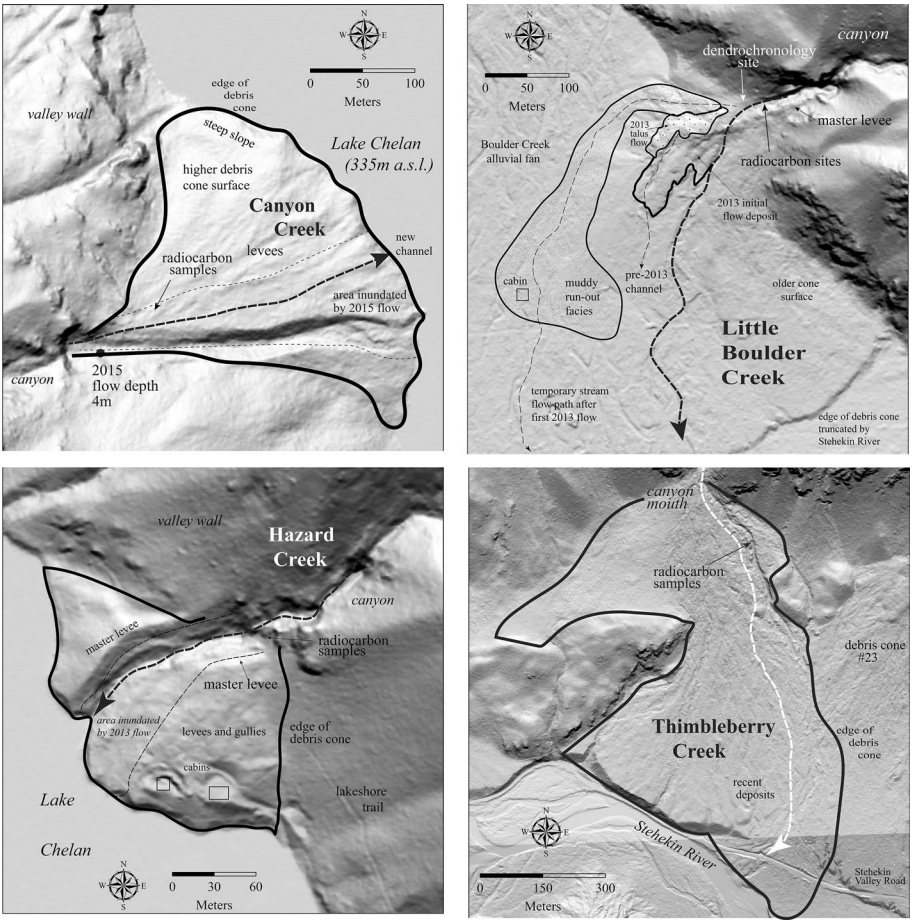

Fig. 2 Lidar hillsade images of select lower Stehekin Valley debris cones depicting morphological features and radiocarbon sample sites

In steep mountainous terrain, debris flow systems include a source area, transport/erosion zone (torrent channel), and a deposition zone known as a debris cone (Figs. 1 and 2). Debris flows travel down steep mountainsides along first- and second-order streams, moving as viscous flows that erode existing channel deposits when channel slopes are > 10–20º (Benda 1985; Hungr et al. 2014). Channelized debris flows are also known as debris torrents in this region (Slaymaker 1988). Debris cones are often confused with alluvial fans, but are distinguished by several features, including surface slopes > 10°, large levees, boulders, and in some cases, hummocky topography (Clague and Eisbacher 1984). They occur where small canyons open on to wide valley floors and are often development sites in steep terrain because they have low gradients and stand above the floodplains of larger rivers.

Magnitude and frequency of debris flows are controlled by sediment availability, basin area, relief, and other morphometric characteristics (DeScally et al. 2001; Wilford et al. 2004). Bovis and Jakob (1999) found evidence that weathering (sediment)-limited systems have less frequent debris flows than transport-limited systems (Carson and Kirby 1972).

Sediment sources include shallow failures of rock or soil/debris from the slopes of a basin (i.e., hillslope failures), avalanches of debris in a gully or ravine, and collapse of embankments along lower reaches of the transport stream (Clague and Eisbacher 1984). Entrainment of sediment in transport-limited systems occurs via overland and subsurface flow. Santi et al. (2008) found that overland flow was the dominant process in the initiation of 11 debris flows in southern California, rather than subsurface saturation and hillslope failure.

Debris flows are typically triggered by high-intensity, short-duration precipitation events, sustained heavy rainfall, and/or rapid snowmelt (Clague and Eisbacher 1984; Santi et al. 2008; Cannon et al. 2010). Cannon and Gartner (2005) found that most debris flows in the Intermountain West are caused by short-duration convective thunderstorms with a recurrence interval of 2–10 years. Caine (1980) developed the first estimate of a rainfall initiation threshold for debris flows, while in nearby British Columbia Church and Miles (1987) could not find a precipitation threshold due to the importance of antecedent precipitation and land cover. Guzzetti et al. (2008) examined a global database to develop global and regional intensity-duration thresholds. Staley et al. (2017) suggested that the intensity of rainfall at 15-min duration best-predicted debris flows in the western US.

Debris flows are more common after fire disturbance to vegetation and soil (Swanson 1981; Meyer et al. 1995; Cannon et al. 2010; Riley et al. 2013; DeGraff et al. 2015). Medium to high burn intensity fires leads to increased sediment production and runoff by removal of water-absorbing duff and creation of hydrophobic soils that reduce infiltration, (Bovis and Jakob 1999; Cannon et al. 2010). These changes occur immediately after a fire, while loss of root strength and associated hillslope failures may occur several years later.

Most of the south-facing side of the lower Stehekin River Valley at the head of Lake Chelan was burned by wildfires of varying intensity in the past 20 years, as was part of the opposite valley wall (Fig. 3). In the past 15 years, 15 extreme flood events occurred on nine streams (Table 1) and deposited massive amounts of sediment on debris cones occupied by private homes and cabins, a lodge, marina, visitor center, and several businesses. Our goal for this paper is to assist with management of the hazards posed by extreme flood events in this National Recreation Area. Debris flow hazard is directly related to event magnitude (volume), frequency (recurrence interval), and rainfall initiation threshold (Bovis and Jakob 1999; Jakob 2005; Guzzetti et al. 2008). Specific objectives are to characterize the flood hazard type (magnitude) using morphometric and geologic approaches, estimate event frequency with historic and stratigraphic records, and identify the intensity and duration of the precipitation that triggered recent debris flows. We also qualitatively compare the debris flow record with a local fire history.

2 Methods

2.1 Study area

Stehekin Watershed drains 891 km^2 on the east slope of the North Cascade mountains (Fig. 1). Lower Stehekin Valley and upper Lake Chelan are deeply incised into hard, resistant Skagit Gneiss bedrock between McGregor Mountain and Tupshin Peak (Fig. 1; Tabor and Haugerud 1999). Lake Chelan valley is one of the deepest gorges in North America, with local relief > 3000 m from Bonanza Peak to the bedrock floor of the lake. The orientation of the valley is not structurally controlled and appears to have been superimposed on the Chelan Mountains terrane (Waitt 1972). The valley

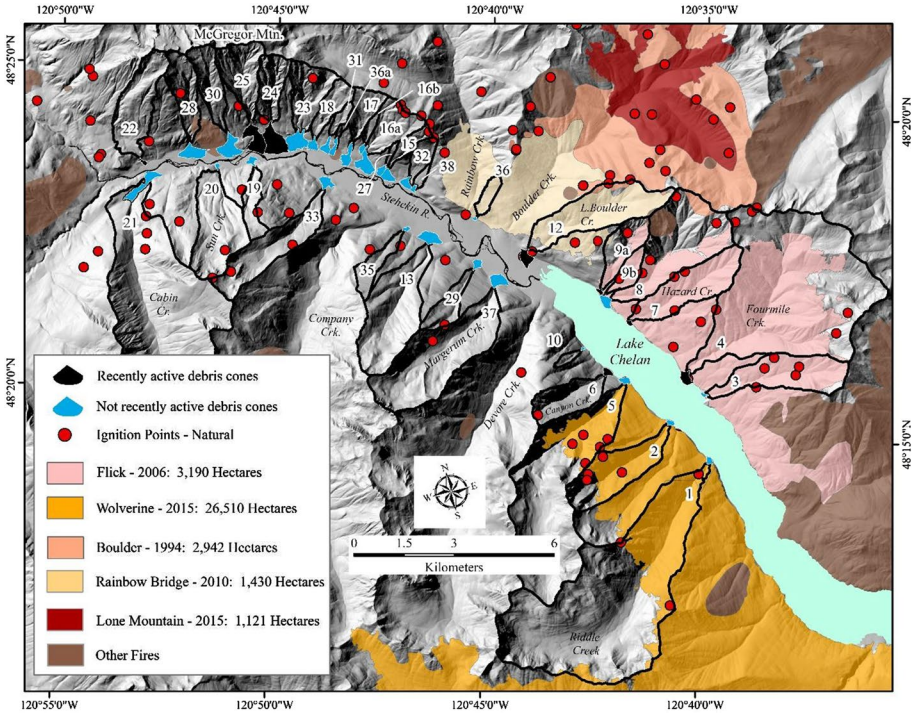

Fig. 3 Recent fires, natural ignition (lightning strike) points, and debris flow basins in lower Stehekin River Valley and the north end of Lake Chelan. Debris cones shown in black carried flows in the past 15 years, while those in blue did not. Basin numbers correspond to those shown in Table 1

has a classic U-shape carved by alpine and continental glaciers with intensely scoured, over-steepened valley walls (Riedel 2017). Surficial deposits are generally thin and discontinuous on the valley walls, but locally glacial drift is 30 m thick. The valley's northwest-southeast orientation creates maximum thermal contrast on the valley walls, influencing land cover and fire and debris flow histories (Figs. 1 and 3).

Lower Stehekin Valley has an arid continental climate but receives more precipitation than adjacent east slope Cascade valleys because of how far west it extends (Fig. 1). The river's headwaters are located on the Pacific crest, down-wind from two large west-slope valleys that funnel large amounts of moisture from the Pacific Ocean. Mean annual precipitation on the valley floor at an elevation of 350 m is 840 mm and mean annual temperature 8.5 ºC. Most precipitation falls as snow between November and March, but late fall and late spring rain-on-snow events cause large floods. Summer convective thunderstorms are common and can produce intense rainfall and lighting. This hydrologic regime leaves the valley walls prone to debris flows most of the year, particularly after vegetation is disturbed. The primary disturbance is fire since there is no logging or grazing. Steep, straight valley wall stream channels, frequent disturbance of vegetation by fire, and a climate that produces brief periods of intense rainfall and rain-on-snow events combine to produce a considerable hazard from debris flows.

Table 1 Summary of debris flow system morphometric characteristics and recent activity in lower Stehekin River Valley

Stream (aspect)	Basin area (km^2)	Watershed length (km)	Relief (km)	Melton ratio	Stream slope (°)	DC area (m^2)	DC volume (m^3 +/− 3%)	DC slope (°)	Flows since 1998
Debris flow									
7-Hazard (SW)	3.20	3.97	1.84	1.03	21	22,858	134,000	14	1
8-Purple (SW)	5.64	4.26	1.86	0.79	21	91,419	698,200	10	
9a-Imus (SW)	1.55	2.58	1.59	1.28	27	24,304	124,400	14	1
9b-S.Imus (SW)	0.70	1.71	1.07	1.22	28	6,415	6,000	8	
12-L. Boulder (SW)	4.13	4.73	1.76	0.87	18	112,547	317,200	11	3
15-Wilson (SW)	0.53	1.75	1.30	1.78	31	100,345	1,031,800	19	
16a-(SW)	1.57	1.88	1.34	1.07	31	244,942	1,392,400	16	
16b-(SW)	0.21	0.72	0.53	1.15	42	34.439	167,500	16	
17 (SW)	1.02	1.61	1.32	1.32	31	128,629	705,100	17	
18 (SW)	0.98	1.84	1.28	1.29	30	83,034	433,500	17	
22-Howard (S)	2.82	3.28	1.98	1.18	31	26,576	57,000	17	
23-(SW)	1.91	2.02	1.60	1.16	27	279,077	2,300,200	15	
24-(SW)	1.44	1.99	1.60	1.33	32	453,028	3,694,100	12	
25-Thimble. (SW)	2.09	2.46	1.68	1.16	29	369,190	1,534,600	15	4
27 (SW) W. Wilson	0.10	0.76	1.20	3.80	31	56,465	81,600	19	
28-SVR (S)	1.67	2.82	1.88	1.48	24	232,414	3,880,400	18	2
30-(SW)	1.55	2.74	1.76	1.42	29	286,724	1,216,000	14	
31-(SW)	0.30	1.20	1.30	2.36	34	79,419	389,200	22	
32-(SW)	0.65	1.48	1.30	1.60	33	74,508	548,340	18	
36-(SW)	0.45	0.48	0.82	1.22	25	10,922	17,700	12	
36a (SW)	0.08	1.31	0.77	2.75	34	59,476	122,300	26	
38 (SW)	0.17	0.80	0.88	2.15	24	25,935	27,500	32	
South average (n = 23)	1.49	2.11	1.39	1.52	29	125,800	1,030,900	17	
2-(NE)	3.33	3.78	2.1	1.13	20	29,921	230,000	12	

Table 1 (continued)

Stream (aspect)	Basin area (km^2)	Watershed length (km)	Relief (km)	Melton ratio	Stream slope (°)	DC area (m^2)	DC volume (m^3 +/− 3%)	DC slope (°)	Flows since 1998
6-Canyon (NE)	1.90	2.49	1.50	1.09	23	52,989	423,600	16	1
10-Onemile (NE)	0.18	0.95	0.79	2.32	39	8,468	30,900	34	
13-Blackberry (NE)	4.78	4.23	1.70	0.78	20	182,339	2,635,500	13	
19-Moon (NE)	0.93	2.21	1.32	1.39	31	54,612	454,400	14	
20-Sun (NE)	3.67	3.30	1.74	0.92	21	18,080	30,200	15	
29-(NE)	1.05	2.31	1.46	1.43	27	60,598	274,700	15	
33-Battallion (NE)	3.25	4.30	1.68	0.93	22	108,971	785,500	11	
35-(NE)	0.93	2.39	1.18	1.23	28	22,738	48,400	9	1
37-Margerum (NE)	6.33	4.89	2.08	0.82	20	151,716	2,078,200	15	1
North average ($n=10$)	2.64	3.09	1.56	1.20	25	69,000	699,100	15	
Debris flood									
1-Riddle (NE)	19.27	8.52	2.05	0.47	13	31,894	78,800	7	
3-Flick (SW)	3.39	4.25	1.79	0.53	19	15,841	46,500	10	
21-Cabin (N)	19.07	8.45	1.82	0.42	7	230,507	604,300	8	
4-Fourmile (SW)	17.76	6.36	2.57	0.61	13	107,935	1,481,500	8	1
5-Castle (NE)	11.02	7.02	2.14	0.64	19	51,578	453,700	10	
DF average $n=3$	14.87	6.9	2.06	0.51	13	96,500	552,800	8	

DC is debris cone and locations of basins are shown in Fig. 3

2.2 Data sources

We used several approaches to understand the magnitude, frequency, and initiation of debris flows, focusing on 37 small streams that reach the lower Stehekin Valley floor or Lake Chelan. These drainage systems have similar climate and geology and most carry snow avalanches (Figs. 1 and 3).

Our main approach to understanding magnitude was to differentiate debris flood from debris flow hazard using basin morphometry and debris cone stratigraphy to determine what type of events dominate each system. Morphometric data included drainage area, relief, watershed length and gradient, and debris cone gradient (Jackson et al. 1987; DeScally et al. 2001; Wilford et al. 2004, and Kovanen and Slaymaker 2008). We measure these characteristics with GIS on a 10 m DEM base from the National Elevation dataset. The morphometry of debris deposits on the valley floor was measured with a 2015 Lidar survey (Table 1; Fig. 2). Debris cone surface gradient was measured as a hand-drawn line perpendicular to surface contours. Automated GIS estimates tend to under-estimate debris cone gradient when compared to field measurements by including some parts of low-gradient terraces, alluvial fans, or floodplains (Kovanen and Slaymaker 2008).

We also measured the volume and depth of several recent flows to further characterize magnitude. Total debris cone volume was measured from Lidar based on the assumption that the adjacent floodplain, alluvial fan, or terrace of the Stehekin River extended as a plane beneath individual cones. Along Lake Chelan, we used the slope of the valley wall adjacent to the debris cone to limit thickness. No suitable subsurface data are available for Lake Chelan. We also estimated the volume of two recent debris flows by comparing 2004 and 2015 Lidar surveys and by field measurements of the thickness and extent of recent flow events at Imus and Little Boulder creeks. Flow depths were based on stains on trees and scour-limits on canyon walls. We defined larger debris flows as those having a volume of ≥ 1000 m^3.

Debris flow frequency was determined by analysis of local records spanning 40 years and by examining deposits on seven debris cones (Meyer et al. 1995). Local records include National Park Service road maintenance reports, interviews with residents, and aerial photographs taken since 1978 (Table 1). The stratigraphic approach focused on natural exposures along active and abandoned debris cone channels and over-emphasizes larger debris flows that overtop master levees at the canyon mouth (Fig. 2). It was near the apex of the debris cone, where streams incise into debris flow deposits, that we found the best exposures. We measured sections and sampled organic material for radiocarbon dating from buried soil surfaces that could be traced laterally for many meters. We improved natural exposures with shallow excavations to minimize the potential for surface contamination, and we sampled large pieces of wood and charcoal from these layers to bracket the age of pre-historic debris flows. We assumed that the debris flow has the same age as the soil organic material it buried. We sent radiocarbon samples to two different laboratories for age determination. Splits of two large pieces of charcoal with minimal evidence of contamination were sent to Direct AMS in Seattle and Beta Analytic in Miami to assess laboratory and sampling error. Both laboratories use atomic mass spectroscopy and similar pre-treatments to determine the raw radiocarbon age.

We extracted cores from large Douglas fir trees within the master levees of Hazard and Little Boulder Creeks near canyon mouths to look for debris flow scars representing smaller events (Arbellay et al. 2010; Fig. 2). Neither site is impacted by snow

avalanches. We mounted the cores on wood molding and sanded to count annual growth rings and identify scars.

We did not systematically review all potential sediment sources for each of the 37 basins, but focused on the seven systems where we conduct stratigraphic investigations using aerial photographs and surveys, soil and landform inventories, and field inspections (Bovis and Jakob 1999; Riedel and Probala 2005; NRCS 2012). We also used field and aerial surveys to identify mode of failure for recent debris flows as either mobilization of deposits in stream channels, from embankments, or from shallow landslides on hillslopes.

Empirical data on rainfall intensity and duration were used to examine precipitation thresholds for several recent debris flows (Guzzetti et al. 2008). We examined the intensity-duration threshold for recent debris flows with precipitation data from the Stehekin weather station, located within 10 km of all 37 debris flow basins (Fig. 1). NOAA radar and satellite estimates of rainfall intensity are also examined (NOAA 2020).

The fire history of the area was obtained from National Park Service records and an ongoing research program (Kopper 2020 written communication). These sources identify the location of natural ignitions (lightning strikes), area burned, fire intensity, and fire history.

2.3 Data analysis

We calculated the Melton ruggedness ratio to separate the 37 systems by dominant hydrogeomorphic process (Melton 1957; 1965). This ratio is determined by dividing basin relief by the square root of drainage area. Previous studies have suggested that a ratio of 0.30 separates floods from debris floods (Jackson et al. 1987), while a value of 0.53–0.66 is thought to separate debris floods from debris flows (Bovis and Jakob 1999; Wilford et al. 2004.) We followed the approach of Wilford et al. (2004) by using basin length and Melton ratio to distinguish debris flow from debris floods (Fig. 4).

Debris flow frequency was determined by radiocarbon ages, tree rings, and NPS records. We calculated recurrence interval (RI) by dividing the oldest debris flow age by the number of events recorded afterward. We considered all the recent flow events on each system as one because they occurred within 15 years of each other, an insufficient time for soil formation. Pooling of the recent events allowed us to include them with the larger events emphasized in the stratigraphic record to estimate frequency.

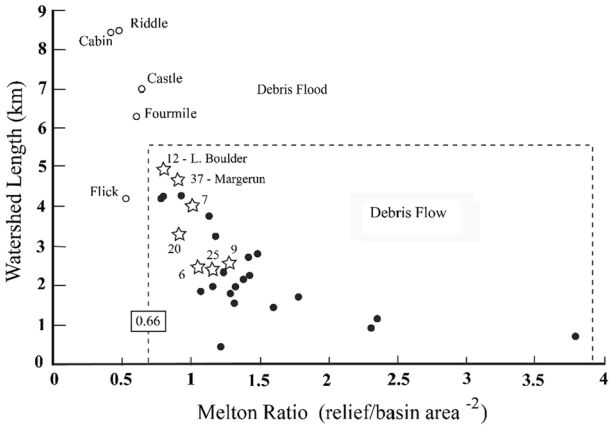

Fig. 4 Plot of basin length compared to Melton ruggedness ratio (relief vs. basin area). Stars indicate systems with radiocarbon records. Dashed box depicts approximate boundary between debris flow and debris flood systems (0.66; Wilford et al. 2004)

We used the online program Oxcal 4.3 (118) to calibrate the raw radiocarbon age estimates (Bronk Ramsey 2009). Table 2 reports the calibrated 2σ age range (95.4%), and the most likely single age based on the highest probability of occurrence. Most of the samples had probabilities of 70–90%, but a few samples are as low as 40% due to multiple peaks in the age distribution.

Rainfall intensity and duration from three Stehekin weather events were compared with previously published global and regional threshold equations. The Guzzetti et al. (2008) study of 2600 events was the focus of our attempt to identify a regional threshold. We did not normalize the intensity data to mean annual precipitation or number of rainy days because these authors showed it did not significantly change their results.

We qualitatively compared the debris flow record with the local fire history. This includes the timing of fires and debris flows, and GIS analysis of the location of natural fire ignitions and the extent and intensity of areas burned within the 37 basins.

2.4 Errors

Our debris cone volume estimates are likely minimums since some debris flow deposits may be inter-fingered with the floodplain sediments at depth, were removed by the Stehekin River, or carried to greater depths in Lake Chelan. An analysis of our debris cone volume method indicated that this introduced an error of ± 3%. Other sources of error in the measurements in Table 1 include the accuracy of the 2004 and 2015 Lidar surveys, and the 1 m resolution NAIP images. We do not quantify these sources of error.

Our recurrence interval estimate has several potential sources of error, including uncertainty in radiocarbon dating and sampling. We primarily sampled near the apices of debris cones on master levees, potentially missing events recorded on older, more distal parts of debris cones. The radiocarbon errors in the AMS technique are shown in Table 2 and range from 20 to 35 years before calibration. For the error in debris flow recurrence interval, we used the average error of 17 samples rounded to the nearest half-century to reflect uncertainty in radiocarbon dating between laboratories. We also spilt two samples and sent them to different laboratories to assess sampling and laboratory errors and found them to be on the order of 100–200 years. The location of most natural exposure near the cone apex predisposed us to look at more recent events and the return time of larger flows that topped master levees to bury soil surfaces. This sample location led us to censor older events buried lower on the debris cones, along with smaller flows contained within the levees and subsequently removed by stream erosion.

Our estimates of precipitation threshold were limited by the lack of weather data at elevation. We used the only weather station data available, which at 500 m elevation is as much as 2000 m below the heads of some of the debris flow basins. We attempted to compare the data from the valley floor with radar and satellite estimates of precipitation but were limited by a small number of events, topographic blocking of ground radar, and the recent deployment of satellites.

Table 2 Radiocarbon ages of buried burned soil surfaces on lower Stehekin River valley debris cones

Sample (Lab #)	Location (bank)—material	Raw ^{14}C age 1 σ error	Median Cal. age (94% confidence)
Little Boulder Creek (#12)			
LBC-7B split sample (D-AMS 017388)	LB low section—charcoal	1664 ± 28	1625 (1690–1448)
LBC-7A split sample (Beta 440399)	Same	1770 ± 30	1813 (1813–1605)
LBC-6 (D-AMS 018278)	LB mid-section—charcoal	217 ± 23	189 (305–modern)
LBC-5 (D-AMS 018279)	LB high section—charcoal	403 ± 23	511 (511–333)
LBC-4B (D-AMS 018280)	RB low—stick	Modern	Modern
LBC-3B split sample (D-AMS 017387)	RB mid-section charcoal	487 ± 26	540 (540–503)
LBC-3A split sample (Beta 440398)	Same	600 ± 30	754 (654–541)
LBC-2 (D-AMS 018281)	RB high section—charcoal	591 ± 22	648 (648–541)
Thimbleberry Creek (#25)			
TC-1 (D-AMS 032871)	RB low section—charcoal	1209 ± 25	1185 (1232–1061)
TC-2 (D-AMS 032870)	RB mid-section—charcoal	445 ± 27	532 (532–473)
TC-5 (D-AMS 032868)	LB top section charcoal	3102 ±35	3387 (3387–3219)
Canyon Creek (#10)			
CC-1 (D-AMS 033926)	LB low section—charcoal	244 ± 23	316 (421–172)
CC-2 (D-AMS 022927)	LB mid-section—charcoal	266 ± 26	326 (429–169)
Sun Creek (#20)			
SC-1 (D-AMS 033928)	LB low section—charcoal	1241 ± 27	1266 (1266–1076)
SC-2 (D-AMS 033929)	LB mid-section—charcoal	1198 ± 28	1184 (1230–1020)
Margerum Creek (#37)			
MC-1 (D-AMS 022930)	RB low-section—charcoal	438 ± 26	529 (529–465)
MC-2 (D-AMS 033931)	RB low section—charcoal	933 ± 26	791 (921–791)
Imus Creek (#9a)			
IC-1 (D-AMS 018282)	LB—charcoal	5187 ± 31	5993 (5993–5907)
IC-2 (D-AMS 018283)	LB—charcoal	Modern	

Table 2 (continued)

Sample (Lab #)	Location (bank)—material	Raw ^{14}C age 1 σ error	Median Cal. age (94% confidence)
IC-4 (D-AMS 018284)	RB—charcoal	4102 ± 27	4655 (4810–4522)
IC-5 (D-AMS 018285)	LB canyon—charcoal	98 ± 20	140 (260–26)
Hazard Creek (#7)			
HC-1 (D-AMS 018286)	LB upper section charcoal	1234 ± 22	1262 (1262–1073)
HC-2 (D-AMS 018287)	LB low section—charcoal	1584 ± 34	1550 (1550–1400)
Fourmile Creek (#4)			
FC-1 (D-AMS 018288)	RB terrace charcoal	2101 ± 25	2140 ((2140–2000)

3 Results and discussion

3.1 Debris flow magnitude

We explore the hazard associated with the deposition zones of 37 low-order streams along the steep valley walls of the lower Stehekin River Valley (SRV) on the arid east slope of the North Cascades (Fig. 1). The morphometric characteristics of these drainage systems and their deposits are summarized in Table 1. In sum, they are small (0.2–19.3 km^2), short (0.5–8.5 km), and steep (26° average path slope and 0.8–2.6 km relief). With these characteristics, they are comparable morphometrically with other debris flow (torrent) and debris flood systems analyzed in the region (Jackson et al. 1987; DeScally et al. 2001; Wilford et al. 2004; Kovanen and Slaymaker 2008).

The recent debris flows were 2.5–6.0 m deep in lower canyons and remained several meters thick between master levees. Deposits on debris cones varied from 2.0 m thick on upper cones to 0.1 m where flows were deposited as lobes on distal parts of the cones. These events deposited large volumes of sediment and could be heard across the valley, underscoring the threat they pose. Little Boulder Creek debris cone accumulated 10,000 m^3 of sediment from the three distinct flows between 2010–2015. This represents about 3% of total debris cone volume (Table 1). The September 6, 2013, Imus flow was 24,500 m^3, or about 10% of debris cone volume. We consider the scale of these events comparable to those preserved in the stratigraphic record.

Key characteristics of the basins we used to distinguish debris flow from debris flood hazard include basin area, relief, and length. Five of the larger basins we examined have Melton ruggedness ratios between 0.42 and 0.64 and are likely debris flood systems (Table 1). Wilford et al (2004) defined these as having Melton ratios between 0.30 and 0.66. Figure 4 compares Melton ratio with basin length to further distinguish the dominant hydrogeomorphic process of each system, distinguishing the five debris flood systems from the 32 debris flow systems. The 32 debris flow basins have Melton ratios that range from 0.78–3.80, reflecting their steep nature. These values are comparable to debris flows systems in the northern Coast Mountains, where Melton ratios range from 0.66 to 1.21 (Wilford et al 2004) and in the northern North Cascades where values range from 0.10 to 2.95 (DeScally et al 2001; Fig. 1).

Other morphometric variables can also be used to distinguish the two types of hydrogeomorphic hazards (Clague and Eisbacher 1984; DeScally et al. 2001). The five debris flood systems deposit debris 'fans' with slopes of 7–10°. In contrast, 32 debris 'cones' formed mainly by debris flows have slopes that reach 34° and average 16° (Table 1). Basin size and stream gradient are also useful metrics, but some small basins can produce deposits with slopes typical of 'debris fans' (e.g., Flick Creek, Table 1).

Sedimentology of debris flow deposits confirms the morphometric distinction of debris floods from debris flow systems. For example, the Fourmile Creek debris fan is composed primarily of sub-rounded boulders and cobbles with little matrix of sand and silt deposited as a series of terraces on both sides of the active channel. The Fourmile Creek deposits were left by debris floods also known as hyper-concentrated flows with extreme bedload transport (Benda 1985; Pierson and Costa 1987; Pierson 2005; Wilford et al. 2004). A relatively flat terrace on the northwest end of the debris fan is capped by 37 cm of sandy silt, in contrast to the coarse-grained modern deposits. The silt originated from erosion of thick and lacustrine deposits upstream that we infer were deposited in the waters of Lake Chelan when its surface elevation was higher before the last ice age.

Debris flow deposits tend to be massively bedded, poorly sorted, and have angular clasts up to 2 m in diameter supported by a sandy matrix (i.e., diamicts; Pierson and Costa 1987; Fig. 5). The typical flow deposit from recent events and in the stratigraphic record is 0.5–1 m thick and can contain enough silt and clay to dry into a dense, hard deposit following de-watering (Fig. 2). The recent flows also contain varying amounts of organic material. A 2010 deposit at Hazard Creek consists of about 30% woody debris, while all the ancient debris flow deposits contain little organic material.

Little Boulder Creek exhibits three distinct facies from recent debris flows: angular cobble and boulders with little matrix, poorly sorted diamict, and a 20–30 cm thick bed of sandy silt. The sand and silt were deposited on the distal part of the debris cone and adjacent floodplain as a muddy runout facies (Fig. 2; Meyer et al. 1995). The 2,500 m^3 of angular cobbles and boulders were deposited by the later of two debris flows on September 6, 2013. The flow initiated as a rock-fall 2 km above the debris cone and was mobilized by high streamflow as a talus flow (Varnes 1978). The rocks now fill the upper part of the channel of Little Boulder Creek just below the master levees and will likely deflect future flows to lateral parts of the cone (Fig. 2).

The 32 debris cones in the lower SRV have several surface features that also distinguish them from debris fans like Fourmile Creek. Most have blind channels, levees, large boulders, and occasionally hummocky deposits (Fig. 2). Blind channels represent former stream channels with their heads buried by more recent debris flow deposits. Head-cut channels form where flood water back-cuts up the debris cone toward the apex. Some of the debris cones along Lake Chelan contain perched deposits (terraces) that grade to different lake levels. The surface elevation of the lake has declined about 43 m in the past 10,000 years (Riedel and Cunderla 2015), and we infer that these surfaces were abandoned as the lake level dropped. The terraces typically have flat tops deposited as debris flows entered the lake, and they stand up to 10 m or more above active channels. The flat surfaces end abruptly at the lake edge and have steep slopes created by rapid attenuation of flows as they entered deep lake water (Fig. 2). These debris cone features continue up Stehekin Valley to an elevation of 370 m near McGregor Meadows, the postglacial maximum elevation of Lake Chelan.

Many of the debris cones have master levees that extend from the bedrock canyon mouth onto the debris cone, more-or-less perpendicular to the valley wall (Fig. 2). These semi-permanent levees stand 2 m or more above stream channels and form where debris is deposited as it exits the bedrock canyon. These landforms essentially extend the canyon mouth and distribute debris flow deposits farther out onto the debris cone. A few master levees have multiple ridge crests, including smaller inset levees. Master levees preserve continuous deposition from larger debris flows, a record that allows us to determine debris flow frequency over thousands of years (Table 2; Fig. 5). This stratigraphic setting allowed us to disregard problems associated with distribution of events across a convex-shaped debris cone (Strunk 1992).

3.2 Debris flow frequency

Dendrochronology and organic material in buried soil surfaces (BSS) extend our understanding of debris flow history by thousands of years. Contacts between individual flow events in the stratigraphic record are typically marked by BSS and occasionally by lenses of sand and poorly sorted gravel (Fig. 5). Wood and charcoal are concentrated at the top

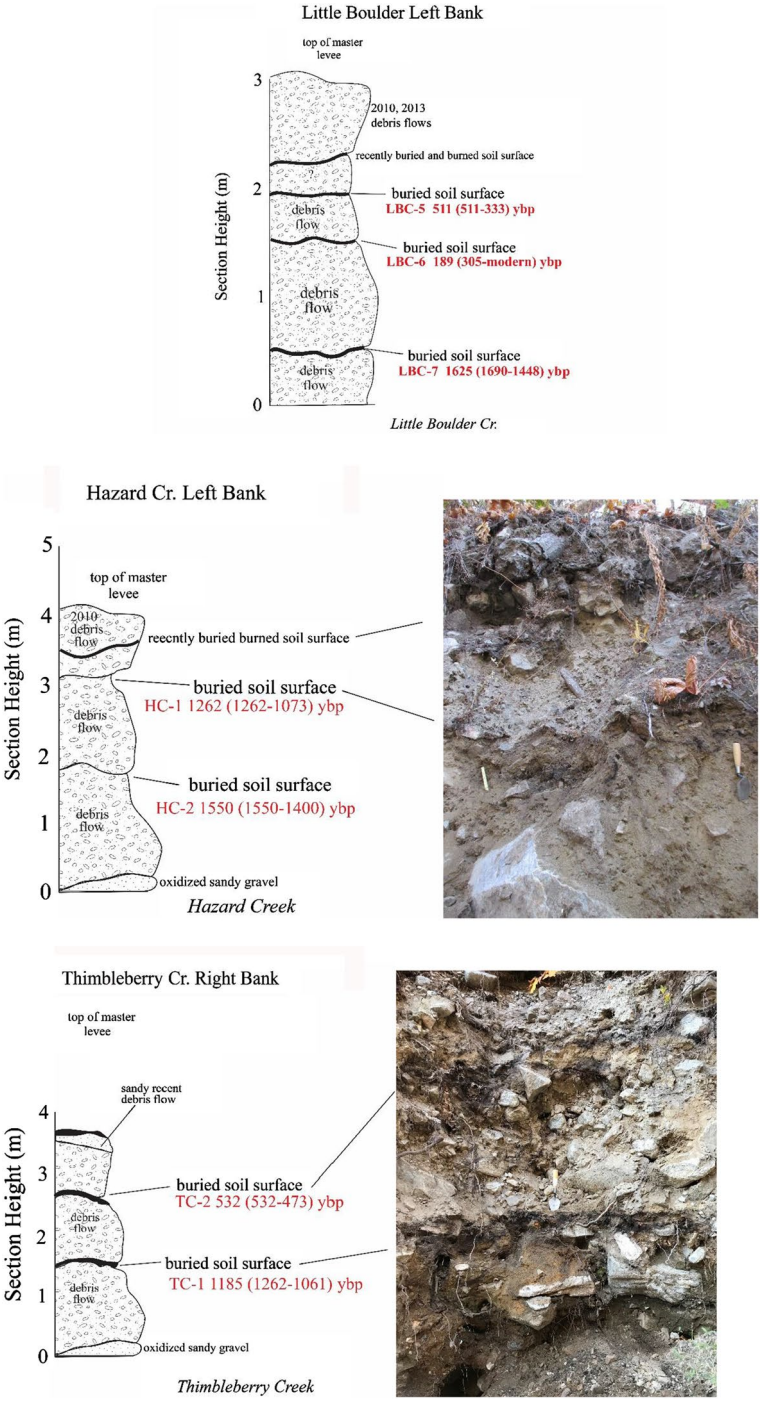

Fig. 5 Stratigraphic diagrams and corresponding photos of upper debris cone exposures on master levees at Little Boulder (top), Hazard (middle), and Thimbleberry (lower) creeks. Radiocarbon ages in red are median age in calibrated years before present, with 95% confidence range in parentheses (Table 2)

of red-stained Bs horizons in the buried soils, representing periods of stability on the cone surface between debris flow events. The BSS can be traced laterally 5–10 m in some cases, essentially following the shape of the master levees (Fig. 2). This stratigraphy shows that larger debris flows add to the height, width, and length of the master levees.

We identified multiple BSS and recovered 26 radiocarbon samples at seven debris cones. Several of the other 25 debris cones have good exposure but no exposed BSS. We selected 22 samples of wood and charcoal for further analyses based on evidence of root contamination and laterally extensive BSS (Table 2). The radiocarbon age estimates obtained from BSS bracket the age of ancient flows but do not provide absolute ages.

Split samples LBC-7 and LBC-3 were sent to different laboratories and returned similar results. Direct AMS laboratory produced estimates 100 and 200 years younger than these sent to Beta Analytic Laboratory (Table 2). We sent the remaining samples to Direct AMS so that more samples could be analyzed. The uncertainty in the accuracy of the age estimate limits out ability to correlate debris flows with fires and other events, but in most cases, this limitation does not preclude the utility of the data for examining the relative history of each debris flow system.

Three of the 22 samples sent in for age determination returned modern ages, meaning that the sample was contaminated. The most likely source of contamination is from tree roots, although sampling procedure, moss, and fungi could also contribute modern carbon. One of the other BSS ages (LBC-6) is inverted and is younger than sample LBC-5 above it (Fig. 5). The contamination issue underscores the problem with sampling near the surface after long intervals between events when tree roots penetrate deeply into past debris flow deposits. Ignoring the modern and inverted ages left 18 reliable radiocarbon age estimates from seven debris cones (Table 2).

We identified four individual ancient debris flow deposits on the left bank of Little Boulder Creek (#12) near the apex of the debris cone, on the inside slope of a master levee (Figs. 2, 3, and 5). Each of the flows was separated by a BSS that provided a radiocarbon age (Table 2). The oldest age of 1625 calendar years before present (ybp; median age) from sample LBC-7 represents a maximum limiting age on the diamict above it (Table 2; Fig. 5). Three more distinct flow deposits are separated by BSS, including the soil buried by the 2013 flow. The BSS in mid-section returned a modern radiocarbon age (LBC-6), and one in the upper section provided an age of 511 ybp (LBC-5), similar to a BSS exposed about 50 m downstream on the right bank. A silty organic layer at the base of the right bank section and two BSS delineate three distinct debris flow deposits. A modern age was obtained from the lower silt bed (LBC-4), and the ages of the mid and upper BSS overlap at 95% confidence (Table 2). The mid-section BSS yielded an age between 654 and 503 ybp based on separate laboratory analyses of a piece of charcoal (LBC-3A and 3B), and charcoal in the upper BSS returned an age of 648–541 ybp (LBC-2; Table 2). The overlapping ages from the two BSS limit the utility of the section for correlating flows with the left bank section and other sites but provide rough upper limiting ages for two debris flow deposits at roughly 648 and 540 ybp.

We extracted two 80 cm long cores from a 1.5 m diameter Douglas fir tree within the master levees of Little Boulder Creek (Fig. 2). The cores revealed an abrupt change in ring growth pattern marked by scarring and deformed, non-parallel rings about 86 years ago. The combined history of Little Boulder Creek debris flows is summarized in Table 3 and in Fig. 6. The time between events during the past 1625 years ranges from 100 to 1000 years, with an average RI of 300 years.

Thimbleberry Creek (#25) has a complex debris cone, with a large volume of sediment perched on a bedrock bench above the Stehekin Valley floor (Fig. 2). Exposures

Table 3 Recurrence interval rounded to nearest half-century for large debris flows on seven drainage systems in lower Stehekin Valley with radiocarbon age records. See text and Table 2 for data on age estimates. Basin percent bare rock surface from NRCS (2012)

Stream (Table 1#)	Basin% rock	Events in calendar years before present (and year A.D.)	Recurrence interval (years)
Little Boulder (12)	12	1625, 648, 540/511, 86 (2010, 2012, 2013)	300
Imus (9)	37	5948, 4641,140, (2013)	1500*
Hazard (7)	7	1550, 1262, (2010)	500
Thimbleberry (25)	26	3387, 1185, 532, (2003, 2006, 2014, 2017)	800
Canyon (6)	42	346, 316, (2015)	150
Margerum (37)	38	791, 529	400
Sun (20)	10	1266, 1184	600
		Average (not including Imus)	450 ± 50

*The Imus recurrence interval is probably smaller than 1500 years due to the 4000-year gap in the record and event-censoring due to the location of the stratigraphic section

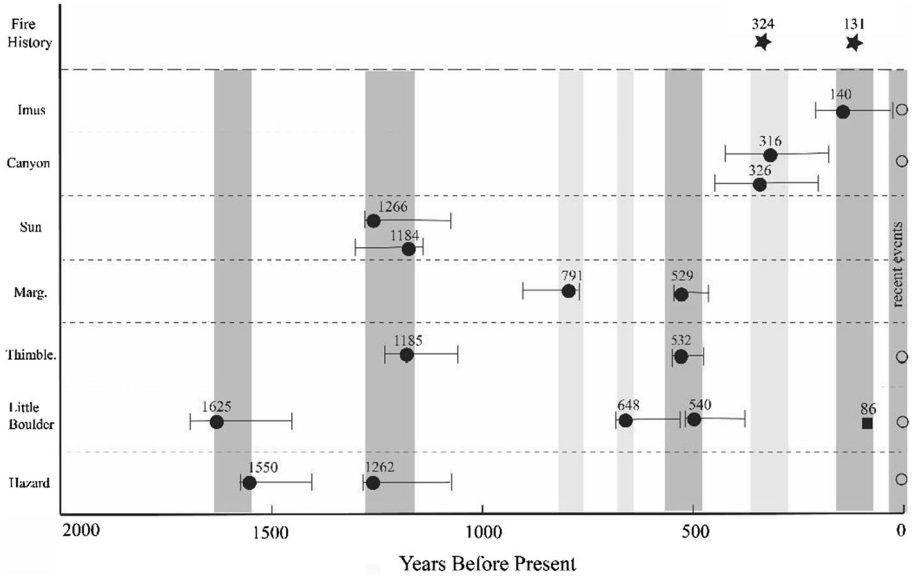

Fig. 6 Age of soil surfaces buried by debris flows during the past 2000 years in the lower Stehekin Valley and northern Lake Chelan. Dark gray shading represents events that occurred on more than one system. Debris flows older than 2000 years were found at Imus Creek (2), Thimbleberry Creek, and Fourmile Creek (Table 3). See Table 2 for recent events. Fire history from Kopper 2020 (personal communication)

on the upper part of the cone revealed multiple debris flow deposits separated by BSS. Near the apex, the left bank is composed of a 10 m exposure of debris flow and fluvial sediments, including a massively bedded diamict 5 m thick. A 20 cm thick organic deposit exposed at the top of the left bank section contains charcoal with a median

radiocarbon age of 3387 ybp. This represents the minimum age limit of the large debris flow exposed on the left bank, and a maximum age for the smaller flows exposed on the right bank (Table 2). Three debris flow deposits exposed on the right bank were separated by two BSS with ages of 1185 and 532 ybp (Figs. 2 and 5). The timespan separating the debris flows since 3387 ybp ranges from 500 to 1200 years, with an average RI of 800 years (Table 3; Fig. 6). Our sample site on the east side of the debris cone apex may not record flows that exited the canyon to the west on the upper bench (Fig. 2). The current hyper-activity of the system and size of the basin also suggest that debris flows are more frequent than the estimated 800-year average RI.

Imus Creek is a steep (27°) stream that deposited a relatively small debris cone near the head of Lake Chelan (#9a; Fig. 3). Several large levees and abandoned stream channels cross its surface. We found two BSS in a gully in the middle part of the debris cone with median ages of 5993 and 4655 ybp that are the oldest debris flow-limiting ages identified in our study (Table 2). Meyer et al. (1995) also found that mid-to-early Holocene debris flow deposits occurred in more distal parts of alluvial fans in Yellowstone National Park. Higher up in the section, beneath the 2013 and an older flow deposit, we observed a 140 ybp BSS that could be traced laterally for several meters (Table 2). We identified four different debris flow deposits on the Imus debris cone, including the 2013 event, spanning about 6000 years (Table 3; Fig. 6). The time between events ranges from 150 to 4500 years, with an average RI of 1500 years. We consider this a rough estimate because of event-censoring caused by our sample location in the middle part of the Imus debris cone and the 4000-year gap in the record.

Hazard Creek enters Lake Chelan about 2 km southeast of Imus Creek (#7; Fig. 3). The modern channel of the creek is deeply incised into the debris cone with matching master levees that contained most of the 2010 flow event (Fig. 2). We measured a well-exposed section at the apex of the debris cone on the left bank, at the base of a small waterfall (Fig. 5). The exposure reveals about 4 m of debris flow deposits, including the 1 m thick 2010 deposit, and two other flow deposits of similar thickness. The diamicts lower in section are separated by two 2–4 cm thick BSS that yielded radiocarbon ages of 1550 and 1262 ybp (Table 2). The three debris flow deposits identified at this site were separated by 300 to 1250 years, with an average RI of 500 years (Table 3; Fig. 6). The average should be considered high because we did not observe smaller flow deposits and had no exposure on the distal flanks of the debris cone. Looking for evidence of smaller flows, we cored the upstream side of an 80 cm diameter Douglas fir tree growing on the left bank of the channel within the master levees (Fig. 2). Two long cores with more than 100 growth rings revealed no debris flow scars, although the tree was deeply scarred by the recent event.

No buried organic material was observed on the well-exposed levees and abandoned channels of Fourmile Creek debris fan (#4; Fig. 3). Two soil test pits on older parts of the fan revealed about 37 cm of fine sand and silt above a BSS formed in a diamict. A large piece of charcoal (FC-1) returned a radiocarbon age of 2140 ybp (Table 2). It is not clear how the silt deposits accumulated, but there has not been recent deposition at the site. The Fourmile Creek debris fan is hazardous because debris floods are large and frequent. They are fed by landslides occuring in a 30 m thick accumulation of glacial till overlying lacustrine sediments about 1 km above the debris fan.

We observed BSS with charcoal in three north-facing debris cones, including Canyon, Margerum, and Sun creeks. We examined Riddle, Battalion, and Blackberry creeks but did not find good exposure or recent flow deposits. At Canyon Creek (#6), 50 m below the debris cone apex, the 2015 debris flow filled a pre-existing channel and eroded a left bank levee to expose three older debris flows. Debris flow deposits are separated by two BSS

that returned ages of 346 and 316 ybp (Fig. 2; Table 2). The 95% confidence calibrated age range of these AMS measurements overlap but the BSSs represent several decades of stability and are traceable laterally for several meters. The time between events ranges from < 100 years to 300 years, with an average RI of 200 years (Table 3). Ten low levees on the north side of the debris cone attest to the active nature of the Canyon Creek debris flow system (Fig. 2).

On the left bank of upper Sun Creek debris cone (#20) stream erosion exposed three debris flow deposits separated by two BSS. Charcoal from the soils returned ages of 1266 and 1184 ybp (Fig. 6). There was no evidence of recent debris flow activity, and two events give a rough average RI of 600 years (Table 3).

Margerum Creek heads in a cirque basin on Tupshin Peak and has built an extensive debris cone (#37; Fig. 3). We observed no recent debris flow deposits at this site but found two BSS exposed on the right bank of the creek near the cone apex. Median radiocarbon ages from charcoal in the soils are 729 and 521 ybp, bracketing the age of two debris flows (Fig. 6). The time between events ranges from 200 to 500 years, with an average RI of 400 years.

Figure 6 summarizes the last 2000 years of debris flow activity in lower Stehekin Valley. This fragmentary record shows debris flows have been common events for the past several millennia. A large event occurred on at least one of the seven debris cones every 200–300 years, close to the estimated average RI of Little Boulder, Canyon, and Margerum creeks (Table 3).

The average RI for larger events on six systems in Stehekin is 450 ± 50 years, an estimate comparable to other regional studies. Jakob (2005) estimated an average regional RI for debris flows of 240 years. Coe et al. (2019) found an RI of 433 ± 44 years for debris flows on nearby Poe Creek. In the northwestern North Cascades foothills, Kovanen and Slaymaker (2008) found the RI for larger debris flows ranged from 481–557 years. Poe Creek has a Melton ratio of 0.45, and all but one of the basins examined by Kovanen and Slaymaker (2008) have Melton ratios ≤ 0.56. These values are within the envelope for debris flood-dominated systems (0.30–0.66; Wilford et al. 2004). Margerum and Little Boulder creeks have ratios of 0.82 and 0.87, respectively, near the 0.66 threshold (Fig. 4).

Smaller debris flows may not be recorded in the stratigraphic record because their deposits are often confined between master levees where they are later eroded by fluvial activity. The dendrochronology record from Little Boulder Creek and debris flows separated by BSS 100 years apart at Sun, Little Boulder, and Canyon creeks indicates that smaller flows have an RI close to 100 years. Bovis and Jakob (1999) report a range in RI of 6 to 60 years for transport-limited and sediment-limited systems in the Coast Mountains, respectively. Their study was based on dendrologic records that captured smaller, more frequent flows. Kovanen and Slaymaker (2008) estimated RI from 67–98 years for small events on 12 debris flood and debris flow systems in the North Cascade foothills. Riley et al. (2013) suggest that post-fire debris flows are smaller and more frequent than debris flows in unburned soils.

Most of the 32 debris flow systems in lower Stehekin Valley are thought to be sediment-limited due to the arid climate and intense glacial scouring of valley walls by the Cordilleran ice sheet (Riedel 2017). Table 3 provides the percent of bare rock in the seven basins with radiocarbon histories and ranges from 42% on Canyon Creek to 7% on Hazard Creek (NRCS 2012). Imus Creek is 37% bare rock and we consider it a sediment-limited system with an RI of ≤ 1500 years (Table 3). At the other ends of the spectrum are the transport-limited debris flow systems on McGregor Mountain, Tupshin Peak, and Castle Rock that

have large sediment sources (Tables 1 and 3; Figs. 1 and 3). Sun and Hazard creeks have 10 and 7% bare rock cover, respectively, and have RIs of 600 and 500 years. We do not have enough data to explore the influence of sediment availability further, but we conclude that transport-limited systems in lower Stehekin Valley have more frequent debris flows because they are more likely to be sensitive to regional thresholds of rainfall (Bovis and Jakob 1999).

Another type of transport-limited system in lower Stehekin Valley and common in the North Cascades are those located in fault zones. Wilson Creek (#15) and Cabin Creek (#21) follow faults, where we infer that heavy jointing and rock alteration provide abundant sediment (Fig. 1). We examined the upper part of the Wilson Creek debris cone but found no buried soils, as expected given the frequency of debris flows in the NPS road maintenance records.

An important element of the ancient record is that it is consistent with modern observations of debris flows clustered in time and space. Multiple debris flow systems were active at ca. 1600, 1200, 500, and 100 ybp, and within the past 15 years (Fig. 6). Three systems had debris flows ca.1200 ybp, and a debris flow at Margerum Creek 791 ybp (Table 3) occurred at about the same time as a debris flood at nearby Poe Creek 752 ybp (Coe et al. 2019). We also uncovered evidence of two debris flows deposited ~ 100 years apart at Little Boulder, Sun, and Canyon creeks. Multiple recent debris flows occurred within a three-year period on some streams. In 2010 (four) and 2013 (two), multiple streams had flows caused by the same storm. These data indicate weather conditions favorable for fires, thunderstorms, and debris flows persist for several decades at a time. This is not surprising given the decadal nature of this region's climate (Mantua et al. 1997; Macdonald and Case 2005; Nelson et al. 2010).

3.3 Precipitation thresholds

A precipitation threshold is the lower limit of rainfall and soil moisture that initiates shallow landslides and debris flows (Reichenbach et al. 1998). This limit is known as the exceedance rainfall threshold, and the main factors are precipitation intensity and duration (Cannon et al. 2010; Segoni et al. 2018).

Debris flows occurred on several of the 32 basins in 2010 and 2013 and were triggered by periods of heavy rainfall in the summer, while a 2015 event occurred in late fall. The records of rainfall that caused these three events are limited to hourly intensity.

- Intense rainfall on August 6, 2010, triggered debris flows on six streams (Table 1), including Hazard, Fourmile, and Little Boulder creeks. Peak intensity was 6.9 mm/h and 37 mm fell over 11 h.
- The September 5–6, 2013, debris flows on Imus and Little Boulder creeks occurred following about 24 mm of rainfall in 4 h, with peak intensity 8.9 mm/h.
- A period of prolonged precipitation from October 31 to November 15, 2015 produced 121 mm of precipitation, some as snow, in three regional events. This was followed by 170 mm of rainfall in 78 h on December 6–8 with peak intensity 8 mm/h that led to a debris flow on Canyon Creek the night of December 8–9.

We compare the intensity and duration of these events to previously published minimum rainfall thresholds in Fig. 7. The Guzzetti et al. (2008) global and mountain threshold

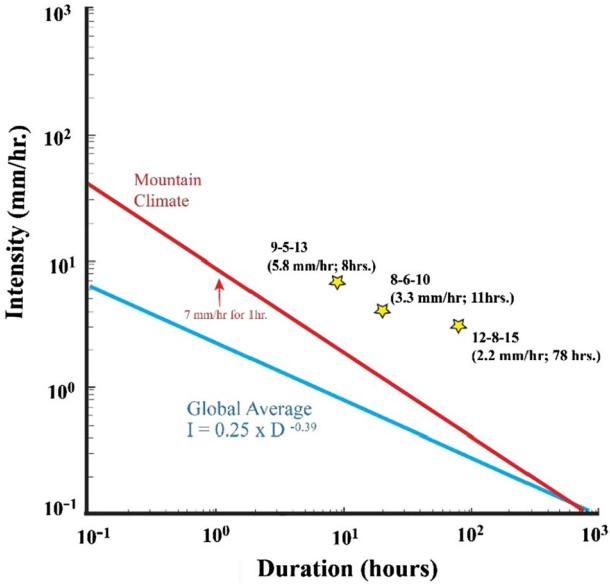

Fig. 7 Minimum rainfall intensity-duration thresholds for initiation of debris flows using global (blue) and mountain (red) datasets (Guzzetti et al. 2008). Recent Stehekin events (yellow stars) fall above both thresholds and were caused by intense summer rainfall in 2010 and 2013, and less intense but longer-duration precipitation in fall 2015

equations were exceeded by all three Stehekin storms. The mountain and global curves suggest that smaller magnitude rainfall events could also trigger debris flows in this valley. Staley et al. (2017) found that 15-min intensity was the best predictor of debris flow activity in the western US. The 15-min intensity of the three storms we examined ranged from 4 to 6 mm/h based on equations in Arkell and Richards (Table 1; 1986).

Antecedent conditions were clearly critical in the 2015 debris flow on Canyon Creek. It is not known why none of the other basins we studied had a debris flow at this time, given the regional nature of the precipitation events. The occurrence of a saturation-induced debris flow sets the Stehekin Valley apart from much of the Intermountain West, where they are rare (Riley et al. 2013). The Stehekin's location on the western edge of this otherwise arid region makes it prone to this type of precipitation (Fig. 1).

It is difficult to determine the frequency of these storms until the National Weather Service updates its storm frequency analyses for Washington (Arkell and Richards 1986). Washington Department of Transportation Design Storm Events (2014) indicates that the RI for the summer 2015 event was about 25 years, while the 2010 and 2013 storms had RIs of 2–10 years. Cannon et al. (2010) also found that this magnitude of storm commonly triggered debris flows in the Intermountain West. Riley et al. (2013) examined 53 recent debris flows in Idaho and Montana and determined that storms with 2 to 25-year RI were responsible. They also found that storms with as small as a 2-year RI triggered debris flows in recently burned areas.

The several hundred-year return periods (RI) calculated from the geologic and dendrochronological records are an order-of-magnitude larger than those of the triggering storms and fires. The fact that storms and fires occur more frequently than debris flows supports the conclusion that many of the Stehekin systems are sediment-limited and that it takes decades or even centuries for an unstable amount of sediment to accumulate in debris flow channels. Fires can accelerate this process because they produce fine-grained sediment in the form of ash (Riley et al. 2013).

3.4 Debris flows and fires

Five fires burned at varying intensities across a combined 352 km^2 near the north end of Lake Chelan from 1994 to 2015 (Fig. 3). The fires burned most of the south-facing valley wall from Rainbow Creek to Flick Creek, including eight of 24 drainage systems. Only three of 13 north-facing basins burned along the north edge of the 263 km^2 Wolverine fire in 2015. Sixty-four natural lightning ignitions occurred on the south-facing valley wall, compared to 45 on the north-facing side. The ignitions and number of fires illustrate that the north-facing side of the valley burns less frequently, but because the vegetation cover is more continuous, fires often burn hotter and are more extensive. The valley's pre-suppression fire RI is about 33 years on south-facing slopes, and 38 years on the north (Kopper 2020 written communication).

Nine of the 11 basins burned in the recent fires spawned 12 of 15 recent debris flows (Table 1). Imus and Canyon creek basins burned partially at low intensity, making it unclear how influential the fires were in their 2013 and 2015 events (Fig. 3). Increased overland runoff due to hydrophobic soils and reduced infiltration due to the combustion of organic soil horizons remain potential factors in several of the recent debris flows (Riley et al. 2013). Fire burn intensity mapping is based mainly on the impact to trees observed from aerial surveys, so 'low intensity' fires may have burned most of the plant litter and duff, decreasing infiltration and increasing runoff. Most of the recent debris flows were failures of deposits in and along channels, and not large hillslope failures.

The stratigraphic record extends the comparison of fire and debris flow histories back several centuries (Fig. 6). All the BSSs are marked by significant charcoal deposits indicating that fires were prevalent in the landscape at the time of the debris flows, or shortly before (Fig. 6). The 1889 A.D. fire burned much of the lower Stehekin Valley, but Imus Creek and Little Boulder Creek are the only sites with evidence of debris flows at about this time (Fig. 6). A fire in 1696 identified on the southwest flank of McGregor Mountain occurred at the same time as two debris flows on Canyon Creek and a debris flood on Poe Creek (Coe et al. 2019; Kopper 2020 written communication).

The asymmetry in fire, natural ignitions, and debris flow activity in this valley is striking. All but three of 15 recent flows and four-of-five fires occurred on the southwest-facing valley wall. Ebel et al. (2015) found that 78% of debris flows identified in Colorado are from south-facing slopes, while Angillieri (2013) analyzed spatial patterns of debris flow activity in the Andes and discovered that south aspects accounted for 43% of the cells with debris flows. Other studies in western North America failed to identify any strong aspect control over debris flow activity (Cannon et al. 2010).

Even though they have similar bedrock, basin areas, Melton ratios, and relief, the drainage systems with a southerly aspect produced six times the volume of sediment compared to those with a northerly aspect since the end of the last glaciation (Table 1). The strong asymmetry in sediment production is due in-part to the high elevation basins with > 1.6 km of relief heading on McGregor Mountain (Fig. 1; Table 1). The southwest-facing valley wall also has twice the drainage density with 24 systems compared to 12 on the north-facing valley wall (Fig. 3). Mountain slopes with higher drainage density move water and sediment rapidly to the valley floor, particularly when vegetation and soils are disturbed.

4 Conclusions

We examine several aspects of the flood hazard associated with occupation of the depositional zones of 37 steep low-order drainage basins in Lake Chelan National Recreation Area. Our analysis led us to the following conclusions.

Morphometric features were useful to identify 32 small drainage systems as dominated by debris flows. These systems have Melton ruggedness ratios between 0.78 and 3.80 that are comparable to three other regional studies. Five basins with Melton ratios between 0.42 and 0.64 are prone to debris flood hazards.

Master levees at the apices of debris cones provide excellent sites for stratigraphic investigations of debris flow history. The inner slopes of these landforms can provide natural exposure of successive flow deposits stacked one on top of the other and separated by buried soil surfaces. This stratigraphic setting can avoid event-censoring associated with sampling on distal parts of convex debris cone surfaces.

The probability of a small debris flow on one of the 32 debris flow streams in any given year is 0.01 (RI = 100), the equivalent of a 100-year flood in terms of frequency. Larger debris flows on six systems studied in detail have an annual probability near 0.002 (RI = 450).

Debris flows can occur at virtually any time of year in this valley, although they are more likely during short, intense summer storms. Precipitation thresholds for the initiation of debris flows are comparable to a global dataset. Recent summer events on seven drainage systems were triggered by storms with a 2 to 10-year recurrence interval with peak intensities of 7–9 mm/h sustained for 8–11 h. Mountain and global thresholds indicate that smaller storms, particularly after fires, could also trigger debris flows.

The debris flow hazard in this valley is asymmetric, with more frequent debris flows from flashy runoff on 24 systems on the fire-prone southwest-facing valley wall. This is particularly true for those systems with abundant sediment supply and high relief, such as those heading on McGregor Mountain.

The recent coincidence of fires and debris flows in this landscape is also observed in the stratigraphic record back to 6,000 ybp. Nearly all buried soil surfaces bracketing debris flow deposits we observed contain charcoal.

Acknowledgements This research was funded by the National Burned Area Emergency Response Program and North Cascades National Park. Special thanks to Nelson Siefkin and Jack Oelfke for their support. We also acknowledge Vicki Gempko, Colin Dowey, Kara Jacobacci, Graham Messe, and Kathryn Ladig for their field support, remote sensing, and GIS expertise. Two anonymous reviewers significantly improved this contribution.

Funding This research was supported by the US National Park Service and the National Burned Area Emergency Response Program.

Compliance with ethical standards

Conflict of interest The authors declare they have no conflict of interest.

References

Angillieri E (2013) Debris flow susceptibility mapping in a portion of the Andes and PreAndes of San Juan, Argentina using frequency ratio and logistic regression models. Earth Sci Res J 17(2):159–167

Arbellay E, Stoffer M, Bollschweiler M (2010) Dendrogeomorphic reconstruction of past debris-flow activity using injured broad-leaf trees. Earth Surf Process Landf 35:399–406

Arkell RE, Richards F (1986) Short duration rainfall relations for the western United States. In: AMS Conference on climate and water management—a critical era. Asheville, North Carolina

Benda LE (1985) Delineation of channels susceptible to debris flows and debris floods. In: International symposium on erosion, debris flow, and disaster prevention, Tsukuba, Japan

Benda LE, Cundy TW (1990) Predicting deposition of debris flows in mountain channels. Can Geotech J 27:409–417

Benda LE, Dunne T (1997) Stochastic forcing of sediment supply to channel networks from landsliding and debris flow. Water Resour Res 33(12):2849–2863

Beverage JP, Culbertson JK (1964) Hyperconcentrations of suspended sediment. J Hydraul Div Am Soc Civ Eng 90:117–128

Bovis MJ, Jakob M (1999) The role of debris supply conditions in predicting debris flow activity. Earth Surf Proc Land 24:1039–1054

Bronk G, Ramsey C (2009) Bayesian analysis of radiocarbon dates. Radiocarbon 51(1):337–360

Caine N (1980) The rainfall intensity-duration control of shallow landslides and debris flows. Geografiska Annaler A 62:23–27

Cannon SH, Gartner JE (2005) Wildfire-related debris flow from a hazards perspective. In: Hungr O, Jakob M (eds) Debris flow hazards and related phenomena. Praxis Springer-Verlag, Berlin, pp 363–385

Cannon SH, Gartner JE, Rupert MG, Michael JA, Rea AH, Parrett C (2010) Predicting the probability and volume of post-wildfire debris flows in the intermountain western United States. Geol Soc Am Bull 122(1/2):127–144

Carson MA, Kirby MJ (1972) Hillslope form and process. Cambridge University Press, London, p 475

Church M, Miles MJ (1987) Meteorological antecedents to debris flow in southwestern British Columbia. In: Costa JE, Wieczorek GF (eds) Debris flows/avalanches: process recognition and mitigation, reviews in engineering geology. Geological Society of America, Boulder VII, pp 63–79

Clague JJ, Eisbacher GH (1984) Destructive mass movements in high mountains: hazard and management. Geological Survey of Canada paper, pp 84–16

Coe JA, Bessette-Kirton EK, Slaughter SL, Rengers FK, Contreras TA, Mickelson KA, Taylor EM, Kean JW, Jacobacci KE, Hanson MA (2019) A 4,000-year history of debris flows in north-central Washington State, U.S.A.: preliminary results from trenching and surficial geologic mapping at the Pope Creek fan. Paper contributed to the 7th International Conference on Debris -Flow Hazards Mitigation, pp 613–620

Cruden DM, Varnes DJ (1996) Landslide types and processes. In: Turner AK and Schuster RL (eds.) Landslides investigation and mitigation. Transportation Research Board, U.S. National Research Council Special Report 247:36–75

DeGraff JV, Cannon SH, Garnter JE (2015) Timing of susceptibility to post-fire debris flows in the western US. Environ Eng Geosci 1(4):277–292

DeScally F, Slaymaker O, Owens I (2001) Morphometric controls and basin response in the Cascade Mountains. Geogr Ann 83A(3):117–130

Dowling CA, Santi PM (2014) Debris flows and their toll on human life; a global analysis of debris-flow fatalities from 1950–2011. Nat Hazards 71:203–227. https://doi.org/10.1007/s11069-013-0907-4

Ebel BA, Rengers FK, Tucker GE (2015) Aspect-dependent soil saturation and insight into debris-flow initiation during extreme rainfall in the Colorado Front Range. Geology 43(8):659–662

Guzzetti F, Peruccacci S, Rossi M, Stark CP (2008) The rainfall intensity–duration control of shallow landslides and debris flows: an update. Landslides 5(1):3–17. https://doi.org/10.1007/s10346-007-0112-1

Hungr O, Evans SG, Bovis M, Hutchinson JN (2001) Review of the classification of landslides of the flow type. Environ Eng Geosci VII:221–238

Hungr O, Lerouielle S, Picarellie L (2014) The Varnes classification of landslide types, an update. Landslides 11:167–194

Jackson LE, Kostaschuk RA, MacDonald GM (1987) Identification of debris flow hazard on alluvial fans in the Canadian Rocky Mountains. In Costa JE, Wieczorek GF (eds.) Debris flows/avalanche: processes, recognition, and mitigation. Reviews of Engineering geology (VII). Geological Society of America

Jakob M (2005) Debris-flow hazard analysis. In: Jakob M, Hungr O (eds) Debris-flow hazards and related phenomena. Springer, Berlin, pp 411–443

Jakob M, Bovis M, Oden M (2005) The significance of channel recharge rates for estimating debris flow frequency and magnitude. Earth Surf Process Landf 30:755–766
Kopper K (2020) Written personal communication on Stehekin Valley fire history
Kovanen DJ, Slaymaker O (2008) The morphometric and stratigraphic framework for estimates of debris flow incidence in the North Cascade foothills, Washington State USA. Geomorphology 99:224–245
MacDonald GM, Case RA (2005) Variation in the Pacific Decadal oscillation over the past millennium. Geophys Res Lett 32:L08703
Mantua NJ, Hare SR, Zhang Y, Wallace JM, Francis RC (1997) A Pacific interdecadal climate oscillation with impacts on salmon production. Bull Am Meteorol Soc 78:1069–1079
Melton MA (1957) And analysis of the relation among elements of climate, surface properties and geomorphology. Office of Naval Reserve Department of Geology Columbia University N.Y. Technical Report 11
Melton MA (1965) The geomorphic and paleoclimatic significance of alluvial deposits in southern Arizona. J Geol 73:1–38
Meyer GA, Wells SG, Hull AJT (1995) Fire and alluvial chronology in Yellowstone National Park: climatic and intrinsic controls on Holocene geomorphic processes. Geol Soc Am Bull 107(10):1211–1230
Nelson D, Abbott M, Steinman B, Polissar P, Stansell N, Ortiz J, Rosenmeier M, Finney, B, and Riedel J (2010) A 6000-yr lake record of drought from the Pacific Northwest. In: Proceedings of the National Academy of Science
NOAA (2020) Data files for specific storms shared by the National Weather Service office in Spokane, Washington
NRCS (2012) Soil survey of North Cascades National Park Service Complex. U.S. Department of Agriculture
Pierson TC (2005) Distinguishing between debris flows and floods from field evidence in small watersheds: U.S. Geological Survey Fact Sheet 2004–3142: 4 p
Pierson TC, Costa JE (1987) A rheologic classification of subaerial sediment-water flows. In Costa JE, Wieczorek (eds.) Debris flows/avalanches—processes, recognition, and mitigation. Reviews in Engineering Geology 7:1–12
Reichenbach P, Cardinali M, De Vita P, Guzzetti F (1998) Hydrological thresholds for landslides and floods in the Tiber River basin (central Italy). Environ Geol 35:146–159. https://doi.org/10.1007/s002540050301
Riedel JL (2017) Deglaciation of the North Cascade Range from the Last Glacial Maximum to the Holocene. Cuadernos de Investigación Geográfica 43(2):467–496
Riedel JL, Cunderla B (2015) Glacial geology of the lake Chelan Area. Field Trip Guide for the Ice Age Floods Institute Fall Field Excursion
Riedel JL, Probala J (2005) Mapping ecosystems at the landform scale in Washington State. Park Sci 23(4):37–42
Riley KL, Bendick R, Hyde KD, Gabet EJ (2013) Frequency-magnitude distribution of debris flows compiled from global data, and comparison with post-fire derbis flows in the western U.S. Geomorphology 191:118–128
Santi PM, deWolfe VG, Higgins JD, Cannon SH, Gartner JE (2008) Sources of debris flow material in burned areas. Geomorphology 96:310–321. https://doi.org/10.1016/j.geomorph.2007.02.022
Segoni S, Piciullo L, Gariano SL (2018) A review of the recent literature on rainfall thresholds for landslide occurrence. Landslides 15:1483–1501. https://doi.org/10.1007/s10346-018-0966-4
Slaymaker O (1988) The distinctive attributes of derbis torrents. Hydrol Sci J 33(6):567–573
Staley DM, Negri JA, Kean, JW, Laber, JM, Tiller AC, Youberg AM (2017) Updated logistic regression equations for the calculation of post-fire debris flow likelihood in the western United States. U.S Geological Survey Open File Report 2016–1106:13 p
Strauch R, Instanbulluoglu E, Riedel JL (2019) A new approach to mapping landslide hazards: a probabilistic, integration of empirical and physically based models in North Cascades USA. Natl Hazards Earth Syst Sci 19:2477–2495
Strunk H (1992) Reconstructing debris flow frequency in the Southern Alps back to 1500 AD using dendrogeomorphological analysis. IAHS 209:299–306
Swanson FJ (1981) Fire and geomorphic processes. In: Mooney HA, Bonnicksen TM, Christensen NL, Lotan JE, Reimers WA (Eds.) Fire regimes and ecosystem properties. U.S. Department of Agriculture Forest Service General Technical Report WO-26:401–420
Swanson FJ, Lienkaemper GW (1978) Physical consequences of large organic debris in Pacific Northwest streams. U.S.D.A. Forest Service General Technical Report PNW-69
Tabor R, Haugerud RA (1999) Geology of the north cascades: a mountain mosaic. The Mountaineers, Seattle, p 143

Varnes DJ (1978) Slope movement types and processes. In: Schuster RL, Krizek RJ (Eds.) Landslides, analysis and control. Special Report 176. Transportation Research Board National Academy of Sciences. Washington, D.C. 11–33

Waitt RB (1972) Geomorphology and Glacial Geology of the Methow Drainage Basin, Eastern North Cascade Range, Washington. Dissertation, University of Washington, Seattle

Washington Department of Transportation. 2014. Highway Runoff Manual—Design Storm Events (Appendix 4C for eastern Washington)

Wilford D, Sakais ME, Innes JL, Sidle R (2004) Recognition of debris flow, debris flood and flood hazard through watershed morphometrics. Landslides 1:61–66